HHS Public Access

Author manuscript

Mol Genet Genomics. Author manuscript; available in PMC 2019 June 01.

Published in final edited form as:

Mol Genet Genomics. 2018 June ; 293(3): 699–710. doi:10.1007/s00438-018-1417-6.

Identification of a Mutation in *CNNM4* by Whole Exome Sequencing in an Amish Family and Functional Link between CNNM4 and IQCB1

Sisi Li[1], **Quansheng Xi**[2], **Xiaoyu Zhang**[1], **Dong Yu**[1], **Lin Li**[2], **Zhenyang Jiang**[1], **Qiuyun Chen**[2,3], **Qing K. Wang**[1,2,3], and **Elias I. Traboulsi**[4]

[1]Key Laboratory of Molecular Biophysics of the Ministry of Education, College of Life Science and Technology, Center for Human Genome Research and Cardio-X Institute, Huazhong University of Science and Technology, Wuhan 430074, China

[2]Center for Cardiovascular Genetics, Department of Molecular Cardiology, Cleveland Clinic Lerner Research Institute, Cleveland, Ohio 44195, USA

[3]Department of Molecular Medicine, Cleveland Clinic Lerner College of Medicine, Department of Genetics and Genome Sciences, Case Western Reserve University School of Medicine, Cleveland, Ohio 44195, USA

[4]Center for Genetic Eye Diseases, Cleveland Clinic Cole Eye Institute, Cleveland, Ohio 44195, USA

Abstract

We investigated an Amish family in which three siblings presented with an early-onset childhood retinal dystrophy inherited in an autosomal recessive fashion. Genome-wide linkage analysis identified significant linkage to marker D2S2216 on 2q11 with a two-point LOD score of 1.95 and a multi-point LOD score of 3.76. Whole exome sequencing was then performed for three affected individuals and identified a homozygous nonsense mutation (c.C1813T, p.R605X) in the cyclin and CBS domain divalent metal cation transport mediator 4 (*CNNM4*) gene located within the 2p14-2q14 Jalili syndrome locus. The initial assessment and collection of the family were performed before the clinical delineation of Jalili syndrome. Another assessment was made after the discovery of the responsible gene and the dental abnormalities characteristic of Jalili syndrome were retrospectively identified. The p.R605X mutation represents the first and probably founder Jalili mutation identified in the Amish community. The molecular mechanism underlying Jalili

Corresponding authors Elias I. Traboulsi, Tel: (216) 444-4363; Fax: (216) 445-2226; traboue@ccf.org (E.I.T.). Qing K. Wang, Tel: +86 2787793502; Fax: +86 2787793502; wangq2@ccf.org or qkwang@hust.edu.cn (Q.K.W.).
S. Li, Q. Xi, X. Zhang, D. Yu and L. Li contributed equally to this work

Compliance with ethical standards

This study was approved by appropriate local institutional review boards on human subject research and conformed to the guidelines set forth by the Declaration of Helsinki.

Conflict of interest All authors declare that they have no conflict of interest.

Ethical approval All procedures performed in studies involving human participants were in accordance with the ethical standards of the IRB on human subject research at Cleveland Clinic and the Ethics Committee on human subject research at Huazhong University of Science and Technology and with the 1964 Helsinki declaration and its later amendments or comparable ethical standards.

Informed consent Written informed consent was obtained from all study subjects.

syndrome is unknown. Here we show that CNNM4 interacts with IQCB1, which causes Leber Congenital Amaurosis (LCA) when mutated. A truncated CNNM4 protein starting at R605 significantly increased the rate of apoptosis, and significantly increased the interaction between CNNM4 and IQCB1. Mutation p.R605X may cause Jalili syndrome by a nonsense-mediated decay mechanism, affecting the function of IQCB1 and apoptosis, or both. Our data, for the first time, functionally link Jalili syndrome gene *CNNM4* to LCA gene *IQCB1*, providing important insights into the molecular pathogenic mechanism of retinal dystrophy in Jalili syndrome.

Keywords

Jalili syndrome; Leber congenital amaurosis (LCA); Early onset childhood retinal; dystrophy; Amish; *CNNM4* mutation; IQCB1

Introduction

The presence of poor vision, nystagmus and light sensitivity from birth is suggestive of a retinal dystrophy (Traboulsi 2010). Achromatopsia, Leber congenital amaurosis (LCA), and Alström syndrome are all associated with this constellation of clinical findings (Michaelides et al. 2006; Traboulsi 2010). Electroretinography is helpful in making the probable clinical diagnosis and reveals evidence of cone and rod dysfunction in LCA and in Alström syndrome, and absent cone, but normal rod responses in achromatopsia (Vedantham et al. 2007; Goodwin 2008; Malm et al. 2008). The presence of systemic abnormalities differentiates LCA from conditions in which the retinal dystrophy is only one sign of a systemic disease resulting from the underlying genetic mutation (Fazzi et al. 2005; Wang et al. 2011; Drivas et al. 2013; Khan et al. 2014; Kumaran et al. 2017).

We studied a two-generation Amish family initially diagnosed with LCA by genome-wide linkage analysis and whole exome sequencing (WES). We identified linkage at chromosome 2p14-2q14 and found a homozygous mutation in the *CNNM4* gene encoding a protein referred to as cyclin and CBS domain divalent metal cation transport mediator 4 (c.C1813T, p.R605X) that causes Jalili syndrome. Re-examination of affected family members more than a decade after initial ascertainment uncovered the dental anomalies which had been overlooked on initial assessment.

Methods

Subjects

The study subjects are 11 members of a family from an Amish community in Ohio. The parents were free of symptoms, but three out of their nine children presented typical clinical features of a neonatal form of retinal dystrophy, judged at the time to be compatible with LCA. Ocular examinations were conducted in 2001 on all members of the family, including three children with evidence of retinal dystrophy. Examinations included Snellen visual acuity testing, slit lamp biomicroscopy, and examination of the lens and fundus after pupillary dilation. Fundus photography was obtained on selected affected individuals. Two

of the affected siblings were reexamined 15 years later and after the identification of the responsible genetic mutation.

This study was approved by the Institutional Review Boards (IRB) on Human Subject Research at the Cleveland Clinic and the Ethics Committee on Human Subject Research at Huazhong University of Science and Technology. Written informed consent was obtained from all study subjects.

Genotyping and linkage analysis

Genomic DNA samples were isolated from peripheral blood samples using standard protocols as described previously (Tian et al. 2004). Genotyping was carried out using either fluorescence or ^{32}P-labeled polymorphic markers as previously described (Wang et al. 2003).

Linkage analysis was performed as described previously (Chen et al. 2004). Two point and multi-point LOD scores were calculated with the Linkage Package (version 5.2) assuming a disease gene frequency of 0.00001, 99% penetrance, a phenocopy rate of 0.0001 and the allele frequencies of markers were 1/n, where n is the number of allele observed.

Whole exome sequencing

WES was carried out using SOLiD 5500XL as described by us previously (Wang et al. 2016). In brief, DNA library preparation and exome capture were performed according to a protocol based on the Fragment Library Preparation 5500 Series SOLiD Systems (Part Number 4460960 Rev. A) and TargetSeq Exome Enrichment System (Part Number MAN0004396). The successfully captured DNA was measured with Invitrogen Qubit dsDNA HS Assay Kit and subjected to standard sample preparation procedures for sequencing with the SOLiD 5500XL platform as recommended by the manufacturer. First, emulsion PCR was performed on an E120 scale using a concentration of 0.6 pM of enriched captured DNA. About 2.2 billion template beads were enriched by SOLiD® EZ Bead Enricher. After modifying the 3’ ends of DNA on the template beads, about 280 million enriched template beads were sequenced per lane on a six-lane SOLiD 5500XL FlowChip.

The data generated by SOLiD 5500xl are in eXtensible SeQuence (XSQ) files. The XSQ files were analyzed by LifeScope Genomic Analysis Software, which contains analysis modules with default parameters. SOLiD® Accuracy Enhancement Tool was used to improve color call accuracy before mapping. Reads were aligned against the human genome reference (UCSC assembly hg19, NCBI build 37) only to a unique position in the reference genome. The aligned reads were converted into the BAM format. Targeted resequencing mapping analysis was used to enrich for reads within whole exon regions. The targeted regions included the exons of 19,911 genes and total 37,262,779 bases in the human genome. We successfully sequenced 93.57%–95.13% of targeted regions to an average depth per individual of 50–55 fold. Variants calls were performed with the SNPs module by taking the mapped and processed SOLiD® System reads, quality values, the reference sequence, and error information of each SOLiD® System slide as its input. Exome sequencing yielded 38,133-40,877variants in the LCA family.

DNA sequence analysis

Sanger sequencing was carried out using Big-Dye v1.0 (ABI) and used to screen for mutational analysis as described previously (Wang et al. 2003).

Plasmids

The expression plasmids for *CNNM4* (pCMV-Tag4A- CNNM4-WT) and *IQCB1* (pCBF-Flag-IQCB1) were described previously (Barbelanne et al. 2013; Yamazaki et al. 2013) and kindly provided by Dr. Hiroaki Miki and Dr. William Y. Tsang, respectively. The *CNNM4* coding region was amplified by PCR analysis using pCMV-Tag4A- CNNM4-WT as the template. The PCR product was digested using restriction enzymes *Hind* III and *Bam*H I (TAKARA, Dalian, China) , then sub-cloned into the multiple cloning site of the pEGFP-N1 vector, generating pEGFP-N1-CNNM4-WT. PCR primers were as follows: F- *Hind* III: 5′-CCCAAGCTTATGGCGCCGGTGGGCGGG-3'and R- *Bam*H I:5′-CGCGGATCCGAGATGGCATTCTCGTGGGAGG-3′. The p.R605X sequence was introduced into pCMV-Tag4A- CNNM4-MUT by PCR amplification. PCR primers mutagenesis included: F- *Bam*H I 5 ′-CGCGGATCCATGGCGCCGGTGGGCGGG-3 ′, R-*Hind* III 5 ′-CCCAAGCTTGGTGTACAGGTAATGGCGGG-3′. The p.R605X sequence was introduced into pEGFP-N1-CNNM4-MUT by PCR amplification. PCR primers mutagenesis included F-*Hind* III 5′-CCCAAGCTTATGGCGCCGGTGGGCGGG-3 ′ and R- *Bam*H I 5′-CGCGGATCCGAGGTGTACAGGTAATGGCGGGC-3′. The *IQCB1* coding region was isolated from pCBF-IQCB1 by digested with restriction enzymes *Sal* I and *Bam*H I and sub-cloned into the multiple cloning site of the p3×FLAG-CMV vector, resulting in p3×FLAG-CMV-IQCB1.

Analysis of apoptosis

Apoptosis assays were carried out with an Annexin V-FITC apoptosis analysis kit (keyGEN, BioTECH, China) using the Beckman Coulter Cytomics FC 500 as described (Luo et al. 2017). Each experiment was repeated at least three times.

Co-immunoprecipitation (Co-IP) analysis

Co-IP analysis was performed as described previously (Huang et al. 2016). The 293T cells were cultured to 80% confluence, and transiently co-transfected with 4 μg of pEGFP-N1-CNNM4-WT or pEGFP-N1-CNNM4-MUT and 4 μg of p3×FLAG-CMV-IQCB1 using Lipofectamine 2000 according to the manufacturer's instructions (Invitrogen, Carlsbad, CA, USA). After 48 h of transfection, cells were harvested and lysed in ice cold cell lysis buffer (Beyotime biotechnology, China) containing 1X cocktail of protease inhibitors. The lysate was centrifuged for 15 min at 13,500 g at 4 °C. Cell extracts were mixed with 2 μg of mouse polyclonal anti-Flag antibody (IgG as negative control) and incubated for 12 h at 4 °C with rotation, followed by another 4 h of incubation with addition of 30 μl of Protein A/G-Sepharose 4B beads (Thermo Scientific, Rockford, IL, USA). The bound proteins complexes were centrifuged at 1000 g for 10 min, and washed 10 times with lysis buffer. The washed pellets were re-suspended in 40 μ1 SDS loading buffer, incubated for 15 min at 100 °C, and electrophoresed through SDS-PAGE as previously described (Zhou et al. 2013). Proteins were transferred onto a PVDF membrane (Millipore, Billerica, MA, USA), and probed with

a goat anti-GFP antibody (1:2000 dilution, ProteinTech, China). After three washes, membranes were incubated with a rabbit anti-goat HRP-conjugated secondary antibody (1:20,000 dilution, Thermo Fisher Scientific, USA) for 2 h at room temperature. Membranes were then imaged using SuperSignal West Pico Chemiluminescent Substrate (Pierce Chemical Co., Rockford, IL, USA) using a ChemiDoc XRS (Bio-Rad Laboratories, Richmond, CA, USA). Each experiment was repeated at least three times.

Results

Clinical findings

Table 1 summarizes the clinical findings on the three affected individuals with typical clinical features of a neonatal form of retinal dystrophy, diagnosed at the time as a form of LCA. Fundus photos are given in Fig. 1. Representative OCTs from patients II-5 and II-8 on their latest visit are shown in Fig. 2. An ERG was not initially obtained in these patients because the retinal degeneration was so advanced that the waveforms were predicted to be severely attenuated.

There are 11 family members (Fig. 3A). Both parents have normal vision and normal teeth. Three children, II-2, II-5 and II-8, were initially diagnosed with LCA, whereas the other six children had normal retinal appearance and vision. The trait in the family appeared to be inherited in an autosomal recessive fashion.

Identification of linkage to 2p14-2q14

Genome-wide linkage analysis with 408 polymorphic markers spanning the whole human genome by every 10 CM identified one chromosomal region around marker D2S2216 linked to the disease in the Amish family (Fig. 3B). Assuming a recessive inheritance model, the highest LOD score of 1.95 was obtained at markers D2S2216 and D2S2972. The peak multi-point LOD score reached 3.76 with D2S2216, which passed the threshold for statistically significant linkage (Fig. 3B). The data suggest that the retinal dystrophy in the Amish family be linked to chromosome 2q11 (Fig. 3B). Haplotype analysis further defined the boundary of the newly identified retinal dystrophy linkage. As shown in Fig. 3A, analysis of recombinant events between the disease trait and each marker at the locus defined the disease locus between markers D2S1772 and D2S1328, which spans a region of about 50 Mb on chromosome 2p14-2q14.

Candidate gene analysis at the 2p14-2q14 locus

The locus between D2S1772 and D2S1328 on 2p14-2q14 contains about 600 genes. Among these genes, *ALMS1* and *MERTK* became candidate genes based on their physical position and functional characteristics. *ALMS1* is the gene responsible for Alström syndrome, whose clinical features include a cone-rod retinal degeneration, with severe light sensitivity (Alstrom et al. 1959). Mutations in *MERTK* have been identified in patients with early-onset retinitis pigmentosa, and can simulate LCA (Gal et al. 2000). All exons and exon-intron boundaries of *ALMS1* and *MERTK* were analyzed by Sanger sequencing and no disease-causing mutation was identified in either gene.

Identification of homozygous mutation p.R605X in *CNNM4* by WES

Since the genome-wide linkage analysis and follow-up candidate gene analysis did not identify the pathogenic mutation responsible for the retinal dystrophy in this family, we performed WES on two affected family members (II-2 and II-5 in Fig. 3A) and one unaffected family member (II-9 in Fig. 3A) using our SOLID 5500xl next generation sequencing platform. Exome sequencing yielded 38,133-40,877 variants in the LCA family (Table 2). Further analysis was then performed by wANNOVAR, a web interface to the ANNOVAR software (http://wannovar.usc.edu/), to annotate all single nucleotide variants (SNVs) (Chang and Wang 2012). Homozygous SNVs were then filtered by excluding the variants which are not shared by the two affected individuals (II-2and II -5), but present in the unaffected individual (II -9) (Table 3). We filtered out SNVs which are present in the dbSNP132 database. We filtered out SNVs which are present in public databases such as the 1000 Genomes Project database (www.1000genomes.org/) and the ExAC database (http://exac.broadinstitute.org/) with a minor allele frequency (MAF) higher than 1‰ (Table 3). The analysis yielded only one variant. By Sanger sequencing verification and co-segregation analysis, we identified the responsible mutation in exon 4 of the *CNNM4* gene (NM_020184; encoding a member of the ancient conserved domain containing protein family) (c.C1813T, p.R605X) that co-segregated with the retinal dystrophy phenotype in this family (Fig. 4A and 4B). The p.R605X mutation does not exist in the ExAC database. The p.R605X was found to be located in the cyclic nucleotide-monophosphate (CNMP) domain of CNNM4, which is highly conserved across species during evolution (Fig. 5).

Follow-up investigation

After the discovery of the *CNNM4* mutation and suspicion of Jalili syndrome, contact was made with the family and examination of the available affected female patients II-5 and II-8 was undertaken. The clinical findings are given in Table 1 and Figures 1 and 2. All three affected siblings but none of the six non-affected ones had severe dental abnormalities that necessitated removal of all of their teeth in their early teens and the fitting of dentures. There were no other systemic abnormalities or diseases. A final diagnosis of Jalili syndrome was hence given to the affected members with homozygous mutations in the *CNNM4* gene.

CNNM4 interacts with IQCB1

The molecular mechanism underlying Jalili syndrome is unknown. Identification of a protein that interacts with the CNNM4 protein will provide novel insights into the molecular mechanism of Jalili syndrome. The NCBI database listed 9 candidate proteins which may interact with CNNM4 (ARL15, CUL3, IQCB1, LRRC39, MBLAC2, PTCH1, PTP4A1, PTP4A2, PTPRO: www.ncbi.nlm.nih.gov/gene/26504). These candidates were identified by affinity capture mass spectrometry (Boldt et al. 2016), but their interactions with CNNM4 were not biochemically confirmed yet. Interestingly, one of the 9 candidates, IQCB1, was associated with LCA (Estrada-Cuzcano et al. 2011; Wang et al. 2011). To demonstrate the interaction between CNNM4 and IQCB1, we transfected 293T cells with p3×FLAG- CMV-IQCB1 together with either pEGFP-N1-CNNM4-WT or pEGFP-N1-CNNM4-MUT, and performed Co-IP analysis. An anti-Flag antibody (recognizing Flag-IQCB1) was used to pull down the potential protein-protein interaction complex, and the complex was detected

using an anti-EGFP antibody recognizing EGFP-CNNM4. The interaction between wild type CNNM4 and IQCB1 was weak, but detectable (Fig. 6A–D). However, robust interaction between the mutant CNNM4 protein with a truncation starting with R605 (missing the C-terminal 170 amino acids) and IQCB1 was easily detected (Fig. 6A–D). These data suggest that the truncation mutant CNNM4 significantly increases the interaction between CNNM4 and IQCB1.

Mutant CNNM4 with a truncation starting at R605 increases apoptosis

We examined the effect of the mutant CNNM4 protein with a truncation starting with codon R605 on apoptosis. Due to difficulties in transfection of retinal pigment epithelial cell lines such as ARPE19 with plasmid DNA, we studied apoptosis in 293T cells. Cells were transfected with the expression plasmids for wild type *CNNM4*, mutant *CNNM4* or empty vector control. Annexin-APC/PI double staining flow cytometry analysis showed that mutant CNNM4 with the truncation significantly increased the rate of apoptosis compared with wild type CNNM4 or vector control ($P<0.05$) (Fig. 7).

Discussion

In the present study of a large Amish family with an infantile-onset retinal dystrophy, genome-wide linkage analysis identified the disease locus on chromosome 2p14-2q14 with a multipoint LOD score of 3.76. Analysis of extended haplotypes localized the gene to about 50 Mb in this region. An initial diagnosis of LCA had been made because the dental abnormalities were overlooked. The affected children had all their teeth pulled and dentures fitted in their teens. The absence of other systemic problems initially supported a diagnosis of LCA, a genetically heterogeneous autosomal recessive retinal dystrophy phenotype, with at least twenty-five causative genes identified to date (Perrault et al. 1996; Marlhens et al. 1997; Freund et al. 1998; Dharmaraj et al. 2000; Sohocki et al. 2000; den Hollander et al. 2001; Dryja et al. 2001; Keen et al. 2003; Janecke et al. 2004; Bowne et al. 2006; den Hollander et al. 2006; Senechal et al. 2006; Mataftsi et al. 2007; Henderson et al. 2009; Ng et al. 2010; Sergouniotis et al. 2011; Wang et al. 2011; Preising et al. 2012; Abu-Safieh et al. 2013; Asai-Coakwell et al. 2013; Wang et al. 2013; Khan et al. 2014; Lazar et al. 2015; Soens et al. 2016) The use of next generation sequencing in the present family identified a homozygous mutation (p.R605X) in the *CNNM4* gene, with strong evidence of pathogenicity, establishing the more precise diagnosis of Jalili syndrome. The mutation p.R605X is located in a functionally important domain of CNNM4, the CNMP binding domain which is highly conserved across species during evolution (Fig. 5). Highly significant linkage with a multipoint LOD score of 3.76 (Fig. 3B) coupled with the results of WES provides strong genetic evidence that mutation p.R605X in CNNM4 is causing Jalili syndrome in this Amish family.

A total of twenty-four *CNNM4* mutations have been documented to cause Jalili syndrome (OMIM #217080), a rare condition consisting of cone-rod dystrophy and amelogenesis imperfecta (AI) (http://jalili.co/CNNM4/cnnm4_muts&stats.htm; Michaelides et al. 2004; Parry et al. 2009; Polok et al. 2009; Jalili 2010; Zobor et al. 2012; Abu-Safieh et al. 2013; Doucette et al. 2013; Luder et al. 2013; Coppieters et al. 2014; Gerth-Kahlert et al. 2015;

Wang et al. 2015; Prasad et al. 2016; Rahimi-Aliabadi et al. 2016; Topcu et al. 2016; Cherkaoui Jaouad et al. 2017). While our initial evaluation of the present family did not identify the AI, reassessment uncovered the severe dental abnormalities that necessitated extraction of all teeth and the fitting of dentures in affected, but not in unaffected siblings or parents.

The molecular mechanism by which *CNNM4* mutations cause retinal dystrophy in Jalili syndrome remains to be identified. CNNM4 is a transporter for Mg^{2+}. It can extrude Mg^{2+} and exchange intracellular Mg^{2+} with extracellular sodium. *CNNM4* knockout mice develop hypomagnesemia. Mutations in *CNNM4* are expected to decrease Mg^{2+} extrusion, which can lead to hypomagnesemia (Yamazaki et al. 2013). Arfuzir et al. (2016) showed that magnesium acetyltaurate (MgAT) significantly reduced ET1-induced retinal cell apoptosis, caspase-3 activation and retinal oxidative stress. Therefore, hypomagnesemia associated with *CNNM4* mutations may cause oxidative stress and retinal cell apoptosis, leading to retinal degeneration and the retinal phenotype of Jalili syndrome. The data presented in Fig. 7 demonstrated that the mutant CNNM4 protein with truncation of the 170 C-terminal amino acids (with p.R605X mutation) induces apoptosis, suggesting that CNNM4 is involved in apoptosis.

One important finding from this study is that CNNM4 interacts with IQCB1 (Fig. 6). Mutations in *IQCB1* cause LCA (Estrada-Cuzcano et al. 2011; Wang et al. 2011; Downs et al. 2016). *IQCB1* is expressed in the photoreceptor connecting cilia (Otto et al. 2005) and is required for mouse photoreceptor outer segment formation (Ronquillo et al. 2016). IQCB1 was shown interact with RPGR and CEP290, which are involved in the pathogenesis of RP and LCA, respectively (Otto et al. 2005; Barbelanne et al. 2015). For the first time, our study functionally links CNNM4 to IQCB1 together, which may explain why some mutations in CNNM4 cause retinal dystrophy in Jalili syndrome.

The molecular mechanism by which *CNNM4* mutation p.R605X causes Jalili syndrome needs to be studied in detail in the future. Nonsense-mediated mRNA decay (NMD) by p. 605X is a potential mechanism. If p.R605X does not cause NMD or NMD is partial, a truncated CNNM4 may also cause the disease by affecting the interaction between CNNM4 and IQCB1 and apoptosis as shown in Figs. 6 and 7. Due to lack of tissue samples form the patients in the Amish family, future knock-in studies with CRISPRA-Cas9 genome editing in cells may be needed to clarify whether p.R605X causes Jalili syndrome by NMD, truncation of CNNM4 or both.

We are aware of another Amish infant with an identical mutation and retinal dystrophy (Schmitt, M., personal communication). While the latter infant does not have teeth yet, it is presumed to have Jalili syndrome. It is probable that that p.R605X in CNNM4 is a founder mutation in the Amish and should be tested for in patients with retinal dystrophy and severe dental abnormalities. Although the exact frequency of the p.R605X in the Amish population is unknown, population-wide study of the p.R605X mutation may identify other carriers in the Amish population.

In summary, this study identifies the first mutation and potentially founder mutation in *CNNM4* that causes Jalili syndrome in the Amish population. Most importantly, our study demonstrates the interaction between CNNM4 and IQCB1, which provides the first link between *CNNM4* and *IQCB1* that causes LCA and retinal dystrophy when mutated, providing important insights into the molecular pathogenic mechanisms of retinal dystrophy in Jalili syndrome.

Acknowledgments

We thank all family members and study subjects for their support of the research and the members of Wang laboratory for help and technical assistance. We thank Dr. Hiroaki Miki for providing plasmid pCMV-Tag4A-CNNM4-WT, and Dr. William Y. Tsang for plasmid pCBF-IQCB1.

Funding This study was supported by the China National Natural Science Foundation grants (91439129, 31430047), 2016 Top-Notch Innovative Talent Development Project from the Bureau of Human Resources and Social Security of Wuhan City, NIH/NHLBI grants R01 HL121358 and R01 HL126729, Hubei Province Natural Science Key Program (2014CFA074), the Chinese National Basic Research Programs (973 Programs 2013CB531101 and 2012CB517801), Hubei Province's Outstanding Medical Academic Leader Program, Specialized Research Fund for the Doctoral Program of Higher Education from the Ministry of Education, and the "Innovative Development of New Drugs" Key Scientific Project (2011ZX09307-001-09); and by an unrestricted grant from Research to Prevent Blindness (EIT).

Abbreviations

WES	Whole exome sequencing
CNNM4	Cyclin and CBS domain divalent metal cation transport mediator 4
LCA	Leber congenital amaurosis
XSQ	eXtensible SeQuence
MAF	Minor allele frequency
SNVs	Single-nucleotide variants
CNMP	Cyclic nucleotide-monophosphate
AI	Amelogenesis imperfect

References

Abu-Safieh L, Alrashed M, Anazi S, Alkuraya H, Khan AO, Al-Owain M, Al-Zahrani J, Al-Abdi L, Hashem M, Al-Tarimi S, Sebai MA, Shamia A, Ray-Zack MD, Nassan M, Al-Hassnan ZN, Rahbeeni Z, Waheeb S, Alkharashi A, Abboud E, Al-Hazzaa SA, Alkuraya FS. Autozygome-guided exome sequencing in retinal dystrophy patients reveals pathogenetic mutations and novel candidate disease genes. Genome Res. 2013; 23:236–247. [PubMed: 23105016]

Alstrom CH, Hallgren B, Nilsson LB, Asander H. Retinal degeneration combined with obesity, diabetes mellitus and neurogenous deafness: a specific syndrome (not hitherto described) distinct from the Laurence-Moon-Bardet-Biedl syndrome: a clinical, endocrinological and genetic examination based on a large pedigree. Acta Psychiatr Neurol Scand Suppl. 1959; 129:1–35. [PubMed: 13649370]

Arfuzir NN, Lambuk L, Jafri AJ, Agarwal R, Iezhitsa I, Sidek S, Agarwal P, Bakar NS, Kutty MK, Yusof AP, Krasilnikova A, Spasov A, Ozerov A, Mohd Ismail N. Protective effect of magnesium acetyltaurate against endothelin-induced retinal and optic nerve injury. Neuroscience. 2016; 325:153–164. [PubMed: 27012609]

Asai-Coakwell M, March L, Dai XH, Duval M, Lopez I, French CR, Famulski J, De Baere E, Francis PJ, Sundaresan P, Sauve Y, Koenekoop RK, Berry FB, Allison WT, Waskiewicz AJ, Lehmann OJ. Contribution of growth differentiation factor 6-dependent cell survival to early-onset retinal dystrophies. Hum Mol Genet. 2013; 22:1432–1442. [PubMed: 23307924]

Barbelanne M, Hossain D, Chan DP, Peranen J, Tsang WY. Nephrocystin proteins NPHP5 and Cep290 regulate BBSome integrity, ciliary trafficking and cargo delivery. Hum Mol Genet. 2015; 24:2185–2200. [PubMed: 25552655]

Barbelanne M, Song J, Ahmadzai M, Tsang WY. Pathogenic NPHP5 mutations impair protein interaction with Cep290, a prerequisite for ciliogenesis. Hum Mol Genet. 2013; 22:2482–2494. [PubMed: 23446637]

Boldt K, van Reeuwijk J, Lu Q, Koutroumpas K, Nguyen TM, Texier Y, van Beersum SE, Horn N, Willer JR, Mans DA, Dougherty G, Lamers IJ, Coene KL, Arts HH, Betts MJ, Beyer T, Bolat E, Gloeckner CJ, Haidari K, Hetterschijt L, Iaconis D, Jenkins D, Klose F, Knapp B, Latour B, Letteboer SJ, Marcelis CL, Mitic D, Morleo M, Oud MM, Riemersma M, Rix S, Terhal PA, Toedt G, van Dam TJ, de Vrieze E, Wissinger Y, Wu KM, Apic G, Beales PL, Blacque OE, Gibson TJ, Huynen MA, Katsanis N, Kremer H, Omran H, van Wijk E, Wolfrum U, Kepes F, Davis EE, Franco B, Giles RH, Ueffing M, Russell RB, Roepman R. An organelle-specific protein landscape identifies novel diseases and molecular mechanisms. Nat Commun. 2016; 7:11491. [PubMed: 27173435]

Bowne SJ, Sullivan LS, Mortimer SE, Hedstrom L, Zhu J, Spellicy CJ, Gire AI, Hughbanks-Wheaton D, Birch DG, Lewis RA, Heckenlively JR, Daiger SP. Spectrum and frequency of mutations in IMPDH1 associated with autosomal dominant retinitis pigmentosa and leber congenital amaurosis. Invest Ophthalmol Vis Sci. 2006; 47:34–42. [PubMed: 16384941]

Chang X, Wang K. wANNOVAR: annotating genetic variants for personal genomes via the web. J Med Genet. 2012; 49:433–436. [PubMed: 22717648]

Chen S, Ondo WG, Rao S, Li L, Chen Q, Wang Q. Genomewide linkage scan identifies a novel susceptibility locus for restless legs syndrome on chromosome 9p. Am J Hum Genet. 2004; 74:876–885. [PubMed: 15077200]

Cherkaoui Jaouad I, Lyahyai J, Guaoua S, El Alloussi M, Zrhidri A, Doubaj Y, Boulanouar A, Sefiani A. Novel splice site mutation in CNNM4 gene in a family with Jalili syndrome. Eur J Med Genet. 2017; 60:239–244. [PubMed: 28246031]

Coppieters F, Van Schil K, Bauwens M, Verdin H, De Jaegher A, Syx D, Sante T, Lefever S, Abdelmoula NB, Depasse F, Casteels I, de Ravel T, Meire F, Leroy BP, De Baere E. Identity-by-descent-guided mutation analysis and exome sequencing in consanguineous families reveals unusual clinical and molecular findings in retinal dystrophy. Genet Med. 2014; 16:671–680. [PubMed: 24625443]

den Hollander AI, Heckenlively JR, van den Born L, de Kok Y, van der Velde-Visser S, Kellner U, Jurklies B, van Schooneveld M, Blankenagel A, Rohrschneider K, Wissinger B, Cruysberg J, Deutman A, Brunner H, Apfelstedt-Sylla E, Hoyng C, Cremers F. Leber congenital amaurosis and retinitis pigmentosa with Coats-like exudative vasculopathy are associated with mutations in the crumbs homologue 1 (CRB1) gene. Am J Hum Genet. 2001; 69:198–203. [PubMed: 11389483]

den Hollander AI, Koenekoop R, Yzer S, Lopez I, Arends M, Voesenek K, Zonneveld M, Strom T, Meitinger T, Brunner H, Hoyng C, van den Born L, Rohrschneider K, Cremers F. Mutations in the CEP290 (NPHP6) gene are a frequent cause of Leber congenital amaurosis. Am J Hum Genet. 2006; 79:556–561. [PubMed: 16909394]

Dharmaraj S, Li Y, Robitaille JM, Silva E, Zhu D, Mitchell TN, Maltby LP, Baffoe-Bonnie AB, Maumenee IH. A novel locus for Leber congenital amaurosis maps to chromosome 6q. Am J Hum Genet. 2000; 66:319–326. [PubMed: 10631161]

Doucette L, Green J, Black C, Schwartzentruber J, Johnson GJ, Galutira D, Young TL. Molecular genetics of achromatopsia in Newfoundland reveal genetic heterogeneity, founder effects and the first cases of Jalili syndrome in North America. Ophthalmic Genet. 2013; 34:119–129. [PubMed: 23362848]

Downs LM, Scott EM, Cideciyan AV, Iwabe S, Dufour V, Gardiner KL, Genini S, Marinho LF, Sumaroka A, Kosyk MS, Swider M, Aguirre GK, Jacobson SG, Beltran WA, Aguirre GD. Overlap of abnormal photoreceptor development and progressive degeneration in Leber congenital

amaurosis caused by NPHP5 mutation. Hum Mol Genet. 2016; 25:4211–4226. [PubMed: 27506978]

Drivas TG, Holzbaur EL, Bennett J. Disruption of CEP290 microtubule/membrane-binding domains causes retinal degeneration. J Clin Invest. 2013; 123:4525–4539. [PubMed: 24051377]

Dryja TP, Adams SM, Grimsby JL, McGee TL, Hong DH, Li T, Andreasson S, Berson EL. Null RPGRIP1 alleles in patients with Leber congenital amaurosis. Am J Hum Genet. 2001; 68:1295–1298. [PubMed: 11283794]

Estrada-Cuzcano A, Koenekoop RK, Coppieters F, Kohl S, Lopez I, Collin RW, De Baere EB, Roeleveld D, Marek J, Bernd A, Rohrschneider K, van den Born LI, Meire F, Maumenee IH, Jacobson SG, Hoyng CB, Zrenner E, Cremers FP, den Hollander AI. IQCB1 mutations in patients with leber congenital amaurosis. Invest Ophthalmol Vis Sci. 2011; 52:834–839. [PubMed: 20881296]

Fazzi E, Signorini SG, Uggetti C, Bianchi PE, Lanners J, Lanzi G. Towards improved clinical characterization of Leber congenital amaurosis: neurological and systemic findings. Am J Med Genet A. 2005; 132A:13–19. [PubMed: 15580639]

Freund CL, Wang QL, Chen S, Muskat BL, Wiles CD, Sheffield VC, Jacobson SG, McInnes RR, Zack DJ, Stone EM. De novo mutations in the CRX homeobox gene associated with Leber congenital amaurosis. Nat Genet. 1998; 18:311–312. [PubMed: 9537410]

Gal A, Li Y, Thompson DA, Weir J, Orth U, Jacobson SG, Apfelstedt-Sylla E, Vollrath D. Mutations in MERTK, the human orthologue of the RCS rat retinal dystrophy gene, cause retinitis pigmentosa. Nat Genet. 2000; 26:270–271. [PubMed: 11062461]

Gerth-Kahlert C, Seebauer B, Dold S, Hanson JV, Wildberger H, Sporri A, van Waes H, Berger W. Intra-familial phenotype variability in patients with Jalili syndrome. Eye (Lond). 2015; 29:712–716. [PubMed: 25613845]

Goodwin P. Hereditary retinal disease. Curr Opin Ophthalmol. 2008; 19:255–262. [PubMed: 18408503]

Henderson RH, Williamson KA, Kennedy JS, Webster AR, Holder GE, Robson AG, FitzPatrick DR, van Heyningen V, Moore AT. A rare de novo nonsense mutation in OTX2 causes early onset retinal dystrophy and pituitary dysfunction. Mol Vis. 2009; 15:2442–2447. [PubMed: 19956411]

Huang Y, Wang Z, Liu Y, Xiong H, Zhao Y, Wu L, Yuan C, Wang L, Hou Y, Yu G, Huang Z, Xu C, Chen Q, Wang QK. alphaB-Crystallin Interacts with Nav1.5 and Regulates Ubiquitination and Internalization of Cell Surface Nav1.5. J Biol Chem. 2016; 291:11030–11041. [PubMed: 26961874]

Jalili IK. Cone-rod dystrophy and amelogenesis imperfecta (Jalili syndrome): phenotypes and environs. Eye (Lond). 2010; 24:1659–1668. [PubMed: 20706282]

Janecke AR, Thompson DA, Utermann G, Becker C, Hubner CA, Schmid E, McHenry CL, Nair AR, Ruschendorf F, Heckenlively J, Wissinger B, Nurnberg P, Gal A. Mutations in RDH12 encoding a photoreceptor cell retinol dehydrogenase cause childhood-onset severe retinal dystrophy. Nat Genet. 2004; 36:850–854. [PubMed: 15258582]

Keen TJ, Mohamed MD, McKibbin M, Rashid Y, Jafri H, Maumenee IH, Inglehearn CF. Identification of a locus (LCA9) for Leber's congenital amaurosis on chromosome 1p36. Eur J Hum Genet. 2003; 11:420–423. [PubMed: 12734549]

Khan AO, Bolz HJ, Bergmann C. Early-onset severe retinal dystrophy as the initial presentation of IFT140-related skeletal ciliopathy. J AAPOS. 2014; 18:203–205. [PubMed: 24698627]

Kumaran N, Moore AT, Weleber RG, Michaelides M. Leber congenital amaurosis/early-onset severe retinal dystrophy: clinical features, molecular genetics and therapeutic interventions. Br J Ophthalmol. 2017; 101:1147–1154. [PubMed: 28689169]

Lazar CH, Kimchi A, Namburi P, Mutsuddi M, Zelinger L, Beryozkin A, Ben-Simhon S, Obolensky A, Ben-Neriah Z, Argov Z, Pikarsky E, Fellig Y, Marks-Ohana D, Ratnapriya R, Banin E, Sharon D, Swaroop A. Nonsyndromic Early-Onset Cone-Rod Dystrophy and Limb-Girdle Muscular Dystrophy in a Consanguineous Israeli Family are Caused by Two Independent yet Linked Mutations in ALMS1 and DYSF. Hum Mutat. 2015; 36:836–841. [PubMed: 26077327]

Luder HU, Gerth-Kahlert C, Ostertag-Benzinger S, Schorderet DF. Dental phenotype in Jalili syndrome due to a c.1312 dupC homozygous mutation in the CNNM4 gene. PLoS One. 2013; 8:e78529. [PubMed: 24194943]

Luo C, Pook E, Tang B, Zhang W, Li S, Leineweber K, Cheung SH, Chen Q, Bechem M, Hu JS, Laux V, Wang QK. Androgen inhibits key atherosclerotic processes by directly activating ADTRP transcription. Biochim Biophys Acta. 2017; 1863:2319–2332. [PubMed: 28645652]

Malm E, Ponjavic V, Nishina PM, Naggert JK, Hinman EG, Andreasson S, Marshall JD, Moller C. Full-field electroretinography and marked variability in clinical phenotype of Alstrom syndrome. Arch Ophthalmol. 2008; 126:51–57. [PubMed: 18195218]

Marlhens F, Bareil C, Griffoin JM, Zrenner E, Amalric P, Eliaou C, Liu SY, Harris E, Redmond TM, Arnaud B, Claustres M, Hamel CP. Mutations in RPE65 cause Leber's congenital amaurosis. Nat Genet. 1997; 17:139–141. [PubMed: 9326927]

Mataftsi A, Schorderet DF, Chachoua L, Boussalah M, Nouri MT, Barthelmes D, Borruat FX, Munier FL. Novel TULP1 mutation causing leber congenital amaurosis or early onset retinal degeneration. Invest Ophthalmol Vis Sci. 2007; 48:5160–5167. [PubMed: 17962469]

Michaelides M, Bloch-Zupan A, Holder GE, Hunt DM, Moore AT. An autosomal recessive cone-rod dystrophy associated with amelogenesis imperfecta. J Med Genet. 2004; 41:468–473. [PubMed: 15173235]

Michaelides M, Hardcastle AJ, Hunt DM, Moore AT. Progressive cone and cone-rod dystrophies: phenotypes and underlying molecular genetic basis. Surv Ophthalmol. 2006; 51:232–258. [PubMed: 16644365]

Ng SB, Buckingham KJ, Lee C, Bigham AW, Tabor HK, Dent KM, Huff CD, Shannon PT, Jabs EW, Nickerson DA, Shendure J, Bamshad MJ. Exome sequencing identifies the cause of a mendelian disorder. Nat Genet. 2010; 42:30–35. [PubMed: 19915526]

Otto EA, Loeys B, Khanna H, Hellemans J, Sudbrak R, Fan S, Muerb U, O'Toole JF, Helou J, Attanasio M, Utsch B, Sayer JA, Lillo C, Jimeno D, Coucke P, De Paepe A, Reinhardt R, Klages S, Tsuda M, Kawakami I, Kusakabe T, Omran H, Imm A, Tippens M, Raymond PA, Hill J, Beales P, He S, Kispert A, Margolis B, Williams DS, Swaroop A, Hildebrandt F. Nephrocystin-5, a ciliary IQ domain protein, is mutated in Senior-Loken syndrome and interacts with RPGR and calmodulin. Nat Genet. 2005; 37:282–288. [PubMed: 15723066]

Parry DA, Mighell AJ, El-Sayed W, Shore RC, Jalili IK, Dollfus H, Bloch-Zupan A, Carlos R, Carr IM, Downey LM, Blain KM, Mansfield DC, Shahrabi M, Heidari M, Aref P, Abbasi M, Michaelides M, Moore AT, Kirkham J, Inglehearn CF. Mutations in CNNM4 cause Jalili syndrome, consisting of autosomal-recessive cone-rod dystrophy and amelogenesis imperfecta. Am J Hum Genet. 2009; 84:266–273. [PubMed: 19200525]

Perrault I, Rozet JM, Calvas P, Gerber S, Camuzat A, Dollfus H, Chatelin S, Souied E, Ghazi I, Leowski C, Bonnemaison M, Le Paslier D, Frezal J, Dufier JL, Pittler S, Munnich A, Kaplan J. Retinal-specific guanylate cyclase gene mutations in Leber's congenital amaurosis. Nat Genet. 1996; 14:461–464. [PubMed: 8944027]

Polok B, Escher P, Ambresin A, Chouery E, Bolay S, Meunier I, Nan F, Hamel C, Munier FL, Thilo B, Megarbane A, Schorderet DF. Mutations in CNNM4 cause recessive cone-rod dystrophy with amelogenesis imperfecta. Am J Hum Genet. 2009; 84:259–265. [PubMed: 19200527]

Prasad MK, Geoffroy V, Vicaire S, Jost B, Dumas M, Le Gras S, Switala M, Gasse B, Laugel-Haushalter V, Paschaki M, Leheup B, Droz D, Dalstein A, Loing A, Grollemund B, Muller-Bolla M, Lopez-Cazaux S, Minoux M, Jung S, Obry F, Vogt V, Davideau JL, Davit-Beal T, Kaiser AS, Moog U, Richard B, Morrier JJ, Duprez JP, Odent S, Bailleul-Forestier I, Rousset MM, Merametdijan L, Toutain A, Joseph C, Giuliano F, Dahlet JC, Courval A, El Alloussi M, Laouina S, Soskin S, Guffon N, Dieux A, Doray B, Feierabend S, Ginglinger E, Fournier B, de la Dure Molla M, Alembik Y, Tardieu C, Clauss F, Berdal A, Stoetzel C, Maniere MC, Dollfus H, Bloch-Zupan A. A targeted next-generation sequencing assay for the molecular diagnosis of genetic disorders with orodental involvement. J Med Genet. 2016; 53:98–110. [PubMed: 26502894]

Preising MN, Hausotter-Will N, Solbach MC, Friedburg C, Ruschendorf F, Lorenz B. Mutations in RD3 are associated with an extremely rare and severe form of early onset retinal dystrophy. Invest Ophthalmol Vis Sci. 2012; 53:3463–3472. [PubMed: 22531706]

Rahimi-Aliabadi S, Daftarian N, Ahmadieh H, Emamalizadeh B, Jamshidi J, Tafakhori A, Ghaedi H, Noroozi R, Taghavi S, Ahmadifard A, Alehabib E, Andarva M, Shokraeian P, Atakhorrami M, Darvish H. A novel mutation and variable phenotypic expression in a large consanguineous pedigree with Jalili syndrome. Eye (Lond). 2016; 30:1424–1432. [PubMed: 27419834]

Ronquillo CC, Hanke-Gogokhia C, Revelo MP, Frederick JM, Jiang L, Baehr W. Ciliopathy-associated IQCB1/NPHP5 protein is required for mouse photoreceptor outer segment formation. FASEB J. 2016; 30:3400–3412. [PubMed: 27328943]

Senechal A, Humbert G, Surget MO, Bazalgette C, Arnaud B, Arndt C, Laurent E, Brabet P, Hamel CP. Screening genes of the retinoid metabolism: novel LRAT mutation in leber congenital amaurosis. Am J Ophthalmol. 2006; 142:702–704. [PubMed: 17011878]

Sergouniotis PI, Davidson AE, Mackay DS, Li Z, Yang X, Plagnol V, Moore AT, Webster AR. Recessive mutations in KCNJ13, encoding an inwardly rectifying potassium channel subunit, cause leber congenital amaurosis. Am J Hum Genet. 2011; 89:183–190. [PubMed: 21763485]

Soens ZT, Li Y, Zhao L, Eblimit A, Dharmat R, Chen Y, Naqeeb M, Fajardo N, Lopez I, Sun Z, Koenekoop RK, Chen R. Hypomorphic mutations identified in the candidate Leber congenital amaurosis gene CLUAP1. Genet Med. 2016; 18:1044–1051. [PubMed: 26820066]

Sohocki MM, Bowne SJ, Sullivan LS, Blackshaw S, Cepko CL, Payne AM, Bhattacharya SS, Khaliq S, Qasim Mehdi S, Birch DG, Harrison WR, Elder FF, Heckenlively JR, Daiger SP. Mutations in a new photoreceptor-pineal gene on 17p cause Leber congenital amaurosis. Nat Genet. 2000; 24:79–83. [PubMed: 10615133]

Tian XL, Kadaba R, You SA, Liu M, Timur AA, Yang L, Chen Q, Szafranski P, Rao S, Wu L, Housman DE, DiCorleto PE, Driscoll DJ, Borrow J, Wang Q. Identification of an angiogenic factor that when mutated causes susceptibility to Klippel-Trenaunay syndrome. Nature. 2004; 427:640–645. [PubMed: 14961121]

Topcu V, Alp MY, Alp CK, Bakir A, Geylan D, Yilmazoglu MO. A new familial case of Jalili syndrome caused by a novel mutation in CNNM4. Ophthalmic Genet. 2017; 38:161–166. [PubMed: 27070327]

Traboulsi EI. The Marshall M. Parks memorial lecture: making sense of early-onset childhood retinal dystrophies--the clinical phenotype of Leber congenital amaurosis. Br J Ophthalmol. 2010; 94:1281–1287. [PubMed: 19825837]

Vedantham V, Jethani J, Vijayalakshmi P. Electroretinographic assessment and diagnostic reappraisal of children with visual dysfunction: a prospective study. Indian J Ophthalmol. 2007; 55:113–116. [PubMed: 17322600]

Wang C, Wu M, Qian J, Li B, Tu X, Xu C, Li S, Chen S, Zhao Y, Huang Y, Shi L, Cheng X, Liao Y, Chen Q, Xia Y, Yao W, Wu G, Cheng M, Wang QK. Identification of rare variants in TNNI3 with atrial fibrillation in a Chinese GeneID population. Mol Genet Genomics. 2016; 291:79–92. [PubMed: 26169204]

Wang H, Wang X, Zou X, Xu S, Li H, Soens ZT, Wang K, Li Y, Dong F, Chen R, Sui R. Comprehensive Molecular Diagnosis of a Large Chinese Leber Congenital Amaurosis Cohort. Invest Ophthalmol Vis Sci. 2015; 56:3642–3655. [PubMed: 26047050]

Wang LJ, Fan C, Topol SE, Topol EJ, Wang Q. Mutation of MEF2A in an inherited disorder with features of coronary artery disease. Science. 2003; 302:1578–1581. [PubMed: 14645853]

Wang X, Wang H, Cao M, Li Z, Chen X, Patenia C, Gore A, Abboud EB, Al-Rajhi AA, Lewis RA, Lupski JR, Mardon G, Zhang K, Muzny D, Gibbs RA, Chen R. Whole-exome sequencing identifies ALMS1, IQCB1, CNGA3, and MYO7A mutations in patients with Leber congenital amaurosis. Hum Mutat. 2011; 32:1450–1459. [PubMed: 21901789]

Wang X, Wang H, Sun V, Tuan HF, Keser V, Wang K, Ren H, Lopez I, Zaneveld JE, Siddiqui S, Bowles S, Khan A, Salvo J, Jacobson SG, Iannaccone A, Wang F, Birch D, Heckenlively JR, Fishman GA, Traboulsi EI, Li Y, Wheaton D, Koenekoop RK, Chen R. Comprehensive molecular diagnosis of 179 Leber congenital amaurosis and juvenile retinitis pigmentosa patients by targeted next generation sequencing. J Med Genet. 2013; 50:674–688. [PubMed: 23847139]

Yamazaki D, Funato Y, Miura J, Sato S, Toyosawa S, Furutani K, Kurachi Y, Omori Y, Furukawa T, Tsuda T, Kuwabata S, Mizukami S, Kikuchi K, Miki H. Basolateral Mg2+ extrusion via CNNM4 mediates transcellular Mg2+ transport across epithelia: a mouse model. PLoS Genet. 2013; 9:e1003983. [PubMed: 24339795]

Zhou B, Si W, Su Z, Deng W, Tu X, Wang Q. Transcriptional activation of the Prox1 gene by HIF-1alpha and HIF-2alpha in response to hypoxia. FEBS Lett. 2013; 587:724–731. [PubMed: 23395615]

Zobor D, Kaufmann DH, Weckerle P, Sauer A, Wissinger B, Wilhelm H, Kohl S. Cone-rod dystrophy associated with amelogenesis imperfecta in a child with neurofibromatosis type 1. Ophthalmic Genet. 2012; 33:34–38. [PubMed: 21728811]

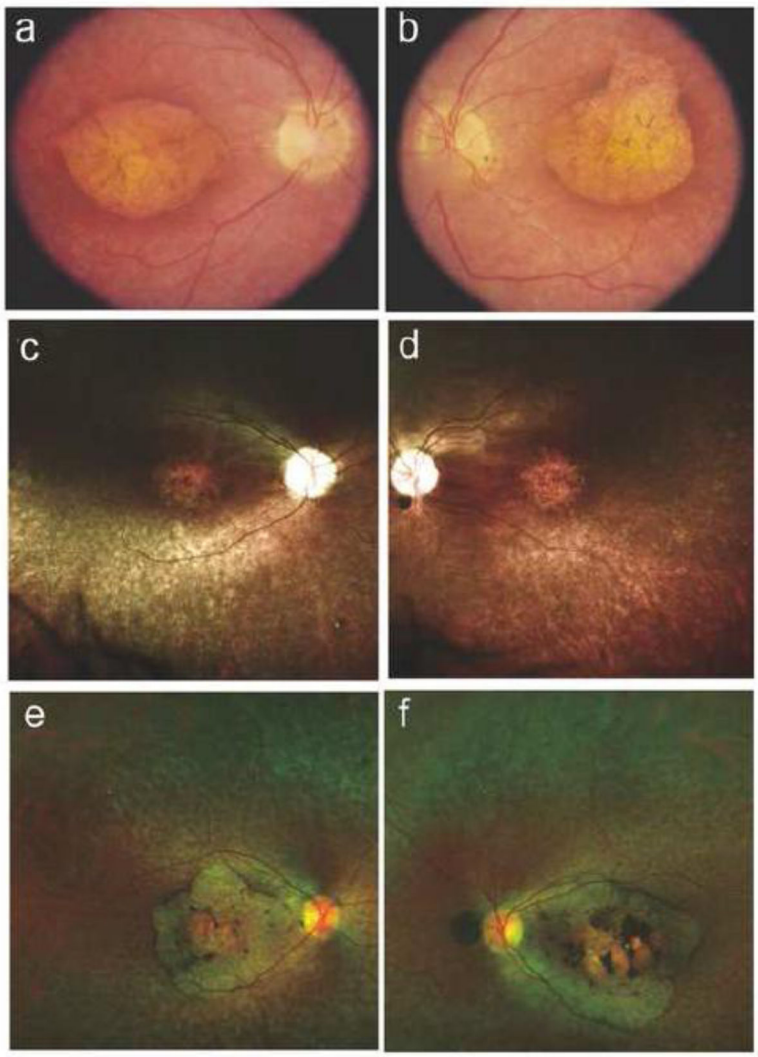

Fig. 1.

Fundus photos of three siblings with Jalili syndrome. Right **a** and left **b** eyes of patient II-2 at age of 20 years. Note the large area of atrophy occupying the macula in both eyes with a pigmented edge. The optic nerve head is pale and the retinal blood vessels are attenuated; there appears to be an area of vitreous condensation inferior to the left optic nerve head. **c** and **d** are from the right and left eyes of patient II-8 at age of 24 years. The optic nerve is atrophic and there is macular atrophy and pigment mottling as well as diffuse atrophic lesions along the vascular arcades and into the periphery; the very white appearance of the nerve head is a photographic artefact. E and F are the posterior pole views of patient II-5 at age of 17 years. The findings appear to represent more advanced stages of what her younger sister's fundus shows in **c** and **d**.

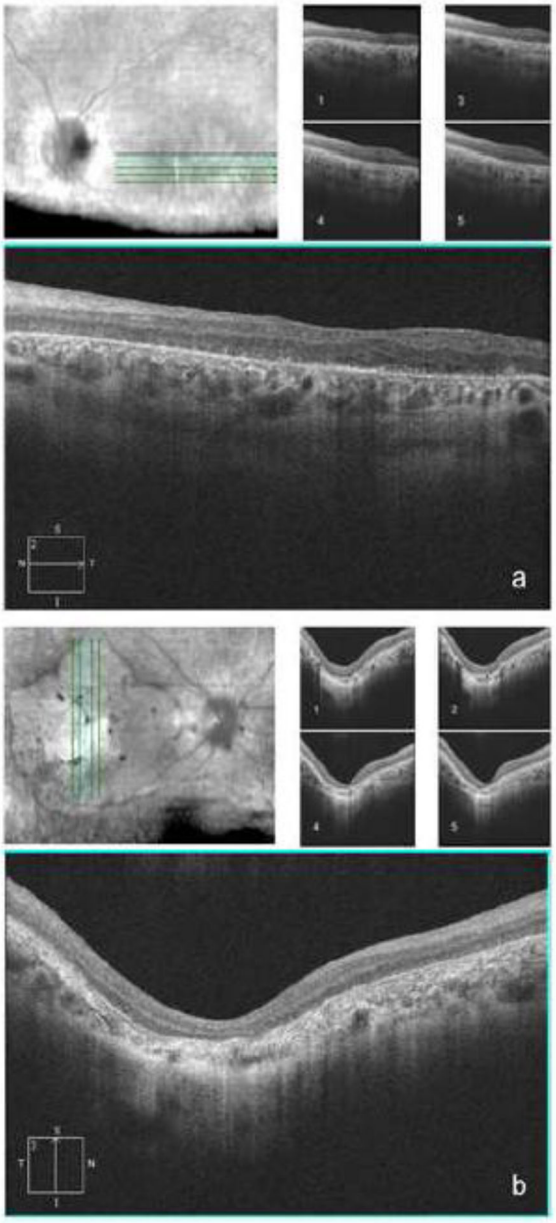

Fig. 2.

Representative OCT. **a** OCT of macular area in the left eye of patient II-8 at age of 24 years. There is almost total loss of the photoreceptor layer. The retinal thickness is reduced. **b** OCT of the macular area of the right eye of patient II-5. Note the presence of a staphyloma as well as the absence of the photoreceptor layer throughout the scanned area.

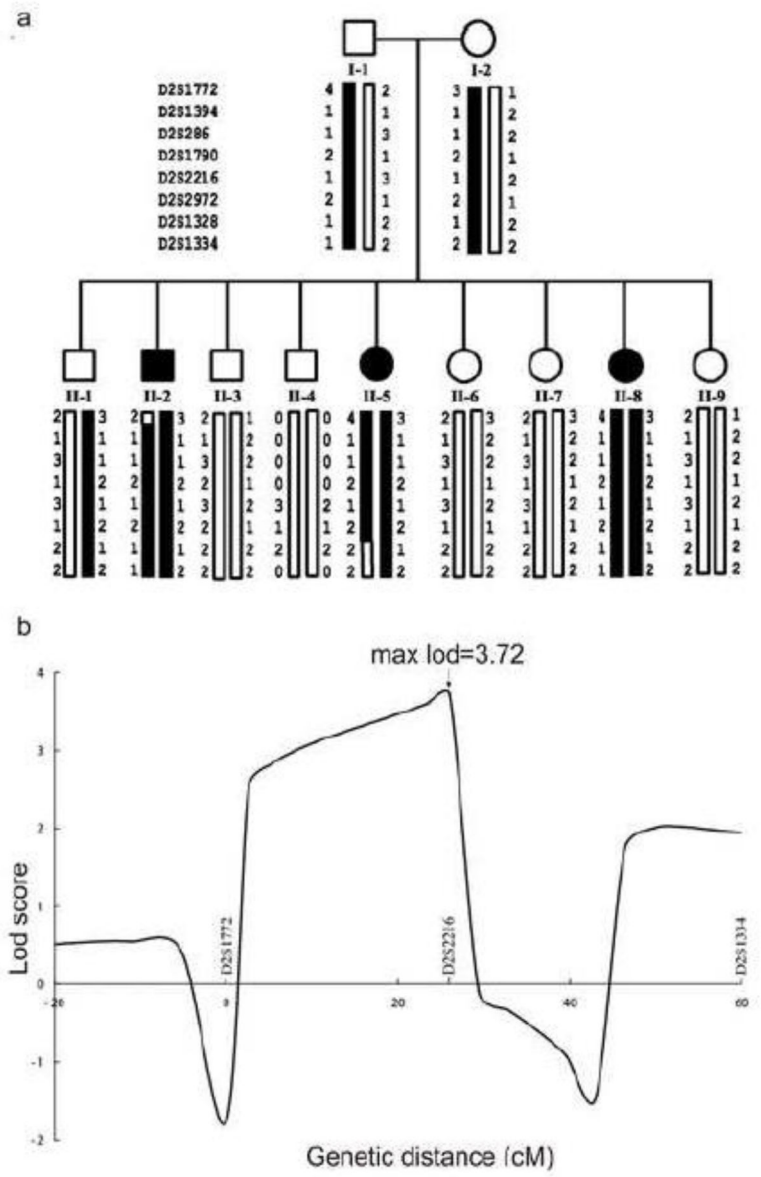

Fig. 3.

Linkage analysis. **a** Pedigree of the Amish family. Individuals affected with Jalili syndrome are indicated by solid symbols; unaffected family members are shown with open symbols. The data from Haplotype analysis are shown under each symbol. The disease locus is defined between markers *D2S1772* and *D2S1328*. **b** Multi-point linkage analysis. The maximum LOD of 3.72 was obtained around D2S2216 (2q11).

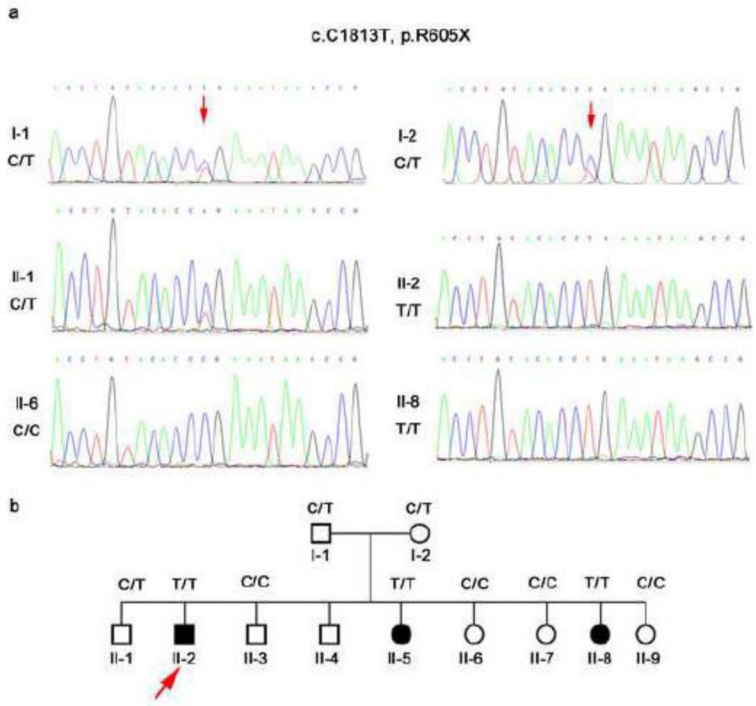

Fig. 4.

Identification of a CNNM4 mutation co-segregating with the disease in the Amish family. **a** Sanger sequencing chromatograms depicting the c.C1813T mutation in *CNNM4* in family members. **b** Mutation (C/T) co-segregates with the disease in the Amish family.

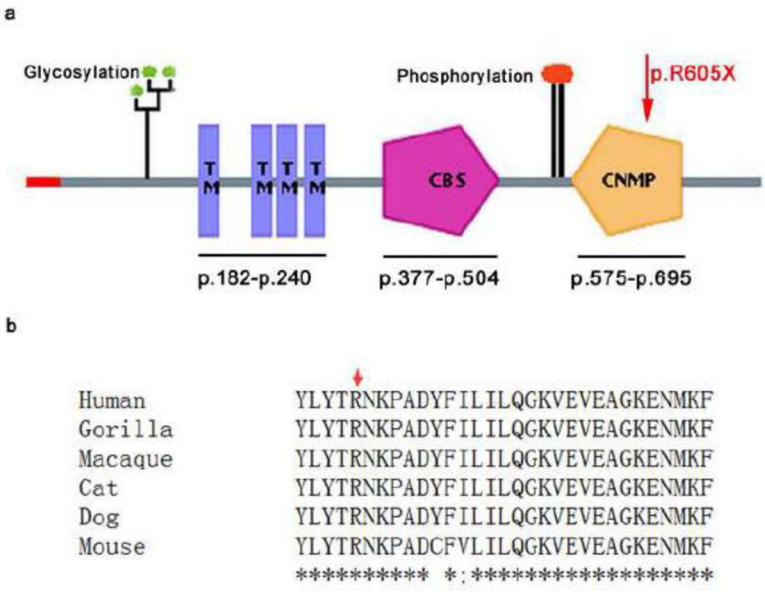

Fig. 5.

Schematic drawing and multiple sequence alignment of the CNNM4 protein. **a** Schematic representation of CNNM4 p.R605X mutation within the CNMP domain (Human Protein Reference Database, http://www.hprd.org/). TM, Transmembrane; CBS, Cystathionine Beta-synthase; CNMP, Cyclic nucleotide-monophosphate binding. **b** Alignment of amino acid sequences of CNNM4 from several vertebrate species, highlighting that amino acid residue R605 and the flanking residues are highly conserved.

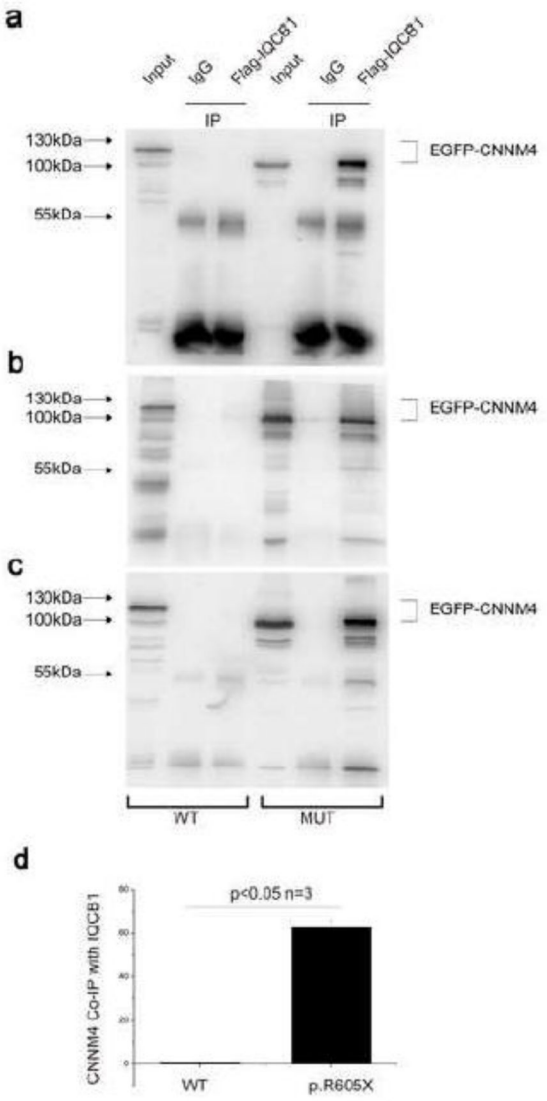

Fig. 6.

The CNNM4 protein interacts with IQCB1 encoded by an LCA-causing gene. **a** Co-IP analysis was performed with extracts from 293T cells co-transfected p3×FLAG-CMV-IQCB1 with pEGFP-N1-CNNM4-WT or pEGFP-N1-CNNM4-MUT. An anti-Flag tag mouse antibody or anti-mouse IgG was used for immunoprecipitation. An anti-EGFP rabbit antibody was used for recognizing EGFP-CNNM4. **b** and **c** shows the data from two other independent Co-IP experiments. **d** The data from a, b and c were scanned, quantified, and plotted. Data were shown as mean ± SEM (*error bars*).

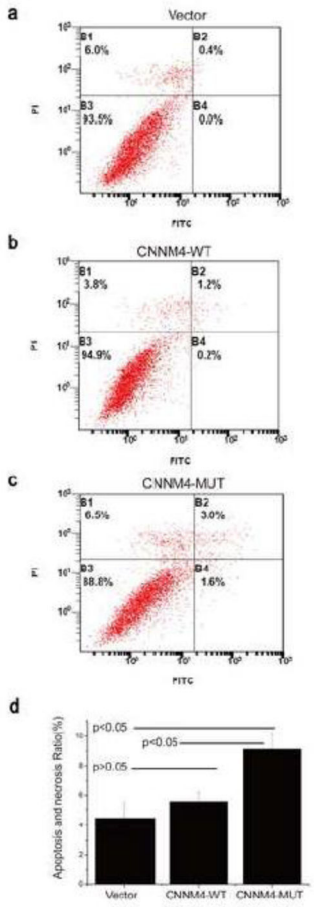

Fig. 7.

A truncated CNNM4 protein at R605 increases apoptosis. **a** Representative flow cytometry images for analysis of apoptosis for control empty vector in 293T cells. b The level of apoptosis for wild type CNNM4, CNNM4-WT. c The level of apoptosis for a mutant CNNM4 protein with truncation starting with codon R605, CNNM4-MUT. **d** The data from a, b and c were scanned, quantified, and plotted. Data were shown as mean ± SEM (*error bars*).

Table 1

Clinical details of affected individuals in present family with Jalili syndrome

Patient(pedigree ID#)	Age at Onset of Symptoms	Age at last Examination(years)	Visual Acuity OU	Fundus findings	Teeth
II-2	Birth	20	20/400	Figure A&B	All extracted. Wears dentures
II-5	Birth	17	6/200	Figure C&D	All extracted Wears dentures
II-8	Birth	24	2/200	Figure E&F	All extracted. Wears dentures

Table 2

Sequencing Details of 3 individuals of LCA family

Sequencing Details	II-2	II-5	II-9
Total target bp	37,262,779	37,262,779	37,262,779
Target bp covered at 1×	95.13%	94.06%	93.57%
Average depth of coverage within targets	50×	55×	52×

Table 3

Filtering of WES variants

Homozygous variants shared by two patients	Homozygous variants not in unaffected member	Not in dbSNP132	MAF <1‰ in public databases			Cosegregation with LCA
Number of SNVs				**Gene**	**Mutation type**	
10531	2174	22	1	*CNNM4*	Stop	√